

# Experimental research of shale pellet swelling in nano-based drilling muds

---

Pašić, Borivoje; Gaurina-Međimurec, Nediljka; Mijić, Petar; Medved, Igor

Source / Izvornik: **Energies**, 2020, 13

Journal article, Published version

Rad u časopisu, Objavljena verzija rada (izdavačev PDF)

<https://doi.org/10.3390/en13236246>

Permanent link / Trajna poveznica: <https://urn.nsk.hr/urn:nbn:hr:169:139685>

Rights / Prava: [Attribution 4.0 International](#)/[Imenovanje 4.0 međunarodna](#)

Download date / Datum preuzimanja: **2024-07-31**






Repository / Repozitorij:

[Faculty of Mining, Geology and Petroleum  
Engineering Repository, University of Zagreb](#)



Article

# Experimental Research of Shale Pellet Swelling in Nano-Based Drilling Muds

Borivoje Pašić \* , Nediljka Gaurina-Međimurec , Petar Mijić  and Igor Medved

Faculty of mining, Geology and Petroleum Engineering, University of Zagreb, 10000 Zagreb, Croatia; ngaumed@rgn.hr (N.G.-M.); petar.mijic@rgn.hr (P.M.); igor.medved@rgn.hr (I.M.)

\* Correspondence: borivoje.pasic@rgn.hr; Tel.: +385-1-553-58-40

Received: 23 October 2020; Accepted: 25 November 2020; Published: 26 November 2020



**Abstract:** The drilling of clay-rich formations, such as shale, is an extremely demanding technical and technological process. Shale consists of mixed clay minerals in different ratios and in contact with water from drilling mud. It tends to swell and cause different wellbore instability problems. Usually, the petroleum industry uses various types of salt and/or polymers as shale hydration inhibitors. The aim of this research was to determine whether nanoparticles can be used as shale swelling inhibitors because due to their small size they can enter the shale nanopores, plug them and stop further penetration of mud filtrate into the shale formation. Swelling of bentonite-calcium carbonate pellets after 2 and 24 h in water and drilling mud (water, bentonite, PAC and NaOH) without nanoparticles and with addition of TiO<sub>2</sub> (0.5, 1 and 1.5 wt%) and SiO<sub>2</sub> (0.5, 1 and 1.5 wt%) nanoparticles was measured using a linear swell meter. Additionally, granulometric analyses of bentonite as well as the zeta potential of tested muds containing nanoparticles were performed. Based on the laboratory research, it can generally be concluded that the addition of SiO<sub>2</sub> and TiO<sub>2</sub> nanoparticles in water and base drilling mud reduces the swelling of pellets up to 40.06%.

**Keywords:** SiO<sub>2</sub> and TiO<sub>2</sub> nanoparticles; wellbore instability; shale hydration; clay swelling; pellets; nano-based drilling mud

## 1. Introduction

Drilling is an extremely demanding technical and technological process during which progress can be slowed down or completely stopped due to many problems. One of the most serious problems that can occur during drilling is borehole instability. This can be defined as any unwanted alteration of the borehole diameter. Consequences of borehole instability can differ, from problems that are relatively easy to solve to problems that require an investment of additional financial resources and extend the time planned for performing an operation. In practice, numerous problems may occur due to borehole instability, such as poor hole cleaning, an unsuccessful cementing job (primary cementing operations), the inability to perform wireline log measurements and problems in tripping drilling string or running down casing [1,2]. Wellbore instability problems during clay-rich formation drilling, such as shale, cost over US\$500–1000 million each year [3]. Figure 1 illustrates different wellbore instability mechanisms during drilling operations.

During the process of wellbore drilling, a certain volume of rock is removed and replaced by a drilling fluid. The required drilling fluid density is dependent on the subsurface formation pressure. Since the density of drilling fluid is lower than the density of the rock, redistribution of stress at the wellbore wall will occur [4–7]. In most cases, before the drilling, a subsurface rock formation is under an in-situ compressive stress state consisting of vertical (overburden) stress ( $\sigma_v$ ) as well as minimum ( $\sigma_h$ ) and maximum ( $\sigma_H$ ) horizontal stress. After drilling, stress redistribution takes place at the vicinity of the wellbore wall causing changes in radial, axial and tangential stress. Regardless of stress alteration

on the wellbore wall, at a certain distance from the wellbore, the rock is still under initial in-situ stresses (Figure 2). If the density of the drilling fluid and resulting pressure is too high or too low, results can be hydraulic fracturing or breakout, respectively, as dominant rock failure mechanisms while drilling. In case of directional or horizontal drilling, wellbore stability strongly depends on orientation of the wellbore with regard to initial in-situ stress [8].

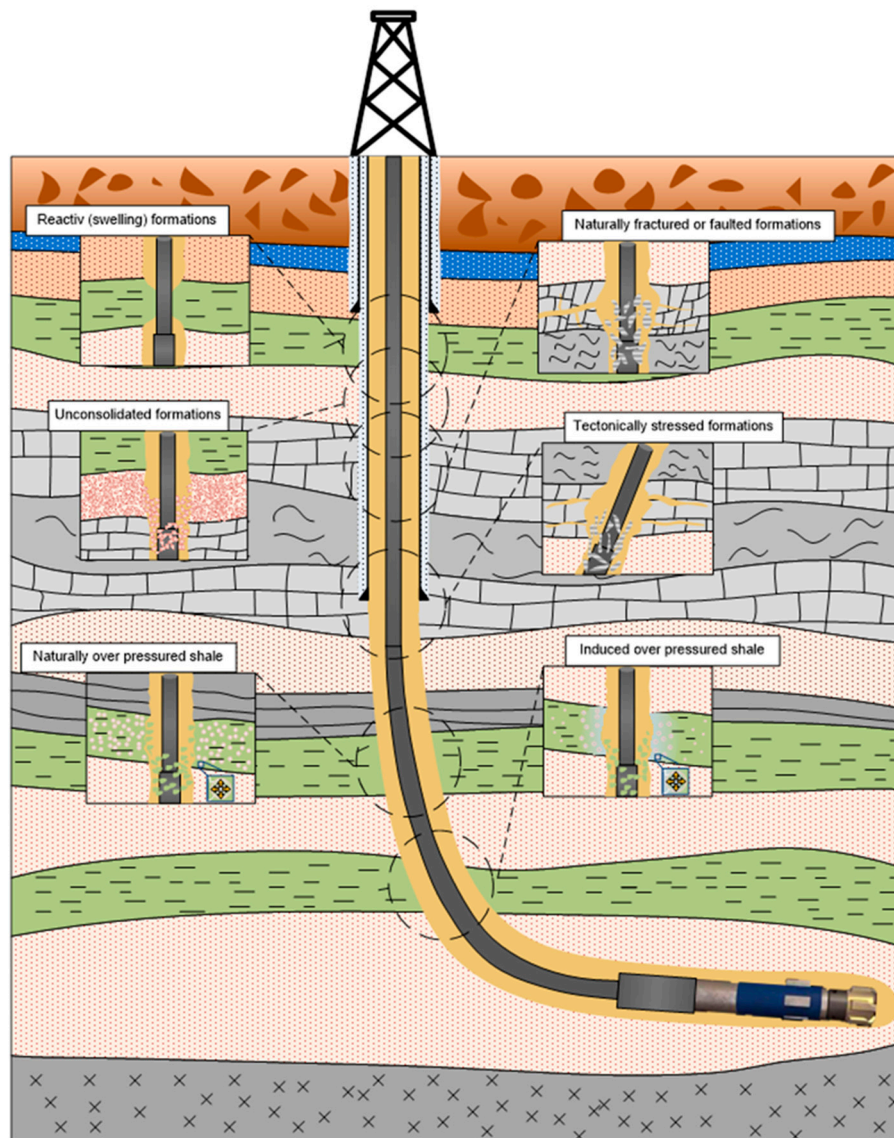


**Figure 1.** Different wellbore instability mechanisms.

Simultaneously with the process of the stress redistribution on the wellbore wall during drilling, a physicochemical interaction between the drilling fluid and the rock will also occur. Physicochemical processes are time-dependent and related to the interaction that takes place between clay formations and water-based muds [9]. If the composition of the drilling fluid is not adequate, various mechanisms may destabilize the wellbore.

Wellbore instability in shale drilling operations can also be time-dependent with a certain delay between exposure of the shale formation to drilling fluid and the first evidence of wellbore instability problems. For example, during drilling of the Laffan and Nahr Umr shale formations on the field west of Abu Dhabi city (UAE), wellbore instability problems occurred after 3–5 days of exposure of the mentioned shale formations [10].

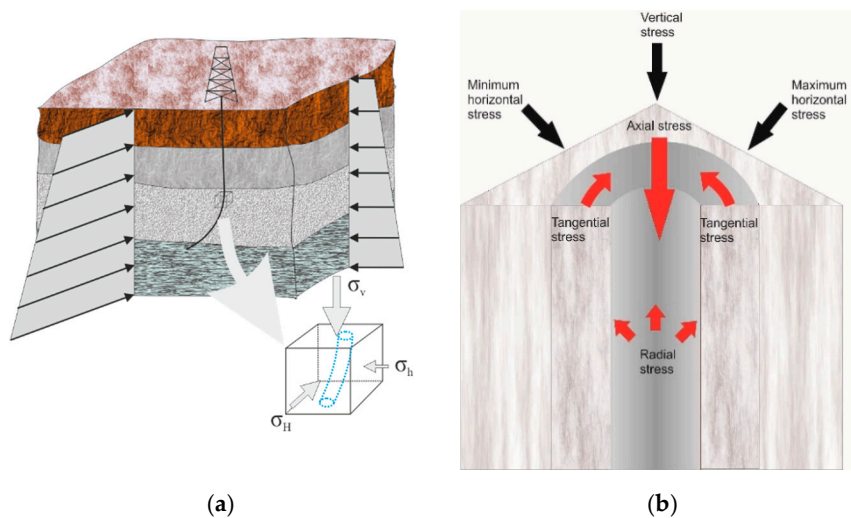


**Figure 2.** Formation in-situ compressive stress before drilling (a) and stress redistribution after drilling (b) [5].

Based on physicochemical interactions, the most important component of the rock is clay. Shale is usually composed of quartz, calcite, clay minerals from the smectite group (most commonly montmorillonite), illite, chlorite and kaolinite in different ratios. Shale also consists of mixed clay minerals in different ratios, which causes the majority of problems during drilling because their swelling behavior is difficult to predict. Each of these clay minerals has a specific crystalline structure, and this also determines the reaction with the drilling mud, especially in water-based muds. In contact with water, clay minerals firstly hydrate and attract water molecules, which can cause dispersion or swelling. Clay swelling increases wellbore instability such as shale sloughing, tight holes and caving and reduces the ability of mud to lift the drilled cuttings [11]. Clay swelling may also cause bit balling and significantly reduce the rate of penetration (ROP), wellbore fill, stuck pipe and high torque values etc. [12,13], and it is responsible for almost 90% of wellbore instability problems [14]. Parkash and Deangeli, 2019, pointed out shale anisotropy as an additional problem related to drilling through shale formations [15]. The shale rock structural anisotropy (existence of weakness planes) makes the process of well design and drilling more complex, especially for wells that are planned and drilled at different angles to formation bedding planes. Today, wellbore instability risk analysis is an integral and indispensable part of modern well design and well trajectory optimization [7,10].

To avoid the physicochemical causes of borehole instability, it is necessary to properly define the composition of the drilling fluid to be used during drilling through a certain rock. Although it has been known for decades that a certain composition of drilling mud provides satisfactory results in wellbore stabilization, recent research suggests that the problem has not been completely solved. The reason for this lies in the rather complex composition of formations like shale, in particular the proportion of different clay minerals and their mutual ratios, as well as their physicochemical characteristics. A significant role in the interaction process between the specific shale formation and water-based drilling fluid is played by the filter cake forming an in-situ semipermeable membrane, and net transfer of water molecules and ions depends on properties of the mentioned semipermeable membrane formed on the face of the shale formation [16].

Various clay hydration inhibitors can be divided into two groups: temporary inhibitors and permanent inhibitors. Temporary inhibitors are used to prevent the hydration of clay minerals and to ensure the stability of the wellbore during the drilling phase, well completion or fracturing. Most commonly, various types of salts such as KCl, NaCl,  $\text{NH}_4\text{Cl}$  and  $\text{CaCl}_2$  are used daily as shale hydration inhibitors. Advances have also been made in the field of the development of permanent inhibitors such as quaternary amine polymers [17,18]. Wellbore stability within the shale formation can be improved by adding a certain amount of wellbore stabilizing agent (WSA) or low-invasion fluid technology (LIFT) in the drilling fluid formulation. Wellbore stabilizing agent causes the creation of a

thin and effective filter cake on face of the shale formation and consequently decreases influx of drilling fluid into shale formation as well as the pressure changes in the nearby wellbore region and increases formation fracture pressure [19,20].

Over the past decade, new materials have been developed and studied for usage as additives in drilling mud, like carboxymethyl starch-grafted-polyacrylamide copolymer [21], poly(styrene-block-acrylamide)/organic montmorillonite nanocomposites, nanocomposite bentonite [22] and Tween 80 (T80)/ZnO nanoparticles as nontoxic additives used in drilling fluid [23]. Despite the large quantity of data available through the different laboratory studies and published papers, wellbore instability problems still exist, and further research work is needed to overcome the wellbore instability problem in the future. Today, such additives can be chopped to nano dimensions and are called nanoparticles. Nanoparticles were first examined in the laboratory, and already there are examples of their successful application in the field, especially for solving the problems associated with drilling. For example, while drilling horizontal sections in Alberta, Canada, in 2014, the operator encountered a problem of lost circulation of the drilling mud, which in some cases amounted to 3 m<sup>3</sup>/100 m of the drilled well. Calcium carbonate nanoparticles in suspension form at a concentration of 0.5 wt% were added to an oil-based drilling mud, and the amount of lost mud decreased by 22–34% [24]. According to Singh et al., 2017, proper sealing of pores and microfractures within a shale formation implies the use of sealing polymer, graphite nanoparticles and microparticles as well as marble particles for plugging wider fractures [25]. The sealing polymer selection process depends on fracture dimensions, temperature, particle size distribution, environmental concern, hydraulics etc. The combination of the nano synthetic polymer and different sizes and types of particles (calcium carbonate, graphite or marble) in oil-based drilling fluid proved successful during drilling through a depleted formation and highly reactive shale formation in Kuwait [26]. Effective sealing of the shale formation and prevention of wellbore instability problems can be achieved through simultaneous use of nanocomposites and lost circulation materials in the drilling fluid formulation [27].

According to literature, the most commonly investigated nanoparticles are SiO<sub>2</sub>, Al<sub>2</sub>O<sub>3</sub>, TiO<sub>2</sub> and Fe<sub>2</sub>O<sub>3</sub>. The particle size of nanoparticles in powder form or nanoparticles in suspensions used in recent laboratory testing varied from 5 [28–30] up to 1205 nm [31]. They were added to the base fluid at various concentrations ranging from 0.1 to 30 wt%. Based on the laboratory research conducted by Gao et al., 2016, and Wang et al., 2018, nanoparticle concentration does not only have an effect on pore pressure alteration in vicinity of the wellbore wall but also slows down this process [32,33]. Due to their large specific area, such particles should be added in lower concentrations [34,35]. Nanoparticles, due to their small dimensions, can enter the nanopores of shale, fill the small space and plug the rock. This results in less chance of water penetration in the rock and thus reduces the hydration process and, ultimately, the swelling of the clay rocks [36]. The results of the most recent laboratory study presented by Hoxha et al., 2019, indicate benefits of using the nanoparticles in drilling fluids to promote wellbore stability through electrostatic and electrodynamic interaction between specific nanoparticles and the shale formation [37]. This interaction is governed by Derjaguin–Landau–Verwey–Overbeek forces, and it is a consequence of surface charge on the face of the shale formation as well as nanoparticle charge, which can be anionic and cationic depending on the manufacturing process. In the real field application, the efficiency of nanoparticles in improvement of the wellbore stability will depend on numerous parameters and conditions such as pH value of drilling fluid, downhole temperature, petrophysical properties of the shale and size and type of the nanoparticles etc.

In addition to wellbore stability, the nanoparticles have the potential to play a very important role in reservoir protection, temperature and pollution resistance of drilling fluids, friction reduction between drill string and casing/rock, hole cleaning during cementing operation, H<sub>2</sub>S removal, enhanced oil recovery etc. [22,38–43]. In the case of using superparamagnetic nanoparticles as weighting agent, more than 90% of those particles can be extracted from the drilling fluid and reused in future drilling operations [22].

To examine the interaction of clay particles with the drilling muds, in this study, pellets were used as a replacement for real clay rock. They were prepared using a compactor and then put in a linear swell meter. Pellets consisted of inert  $\text{CaCO}_3$  and bentonite, which correspond to clay rocks, the swelling rate of which was determined. Instead of using commercial clay inhibitors, in this study,  $\text{SiO}_2$  and  $\text{TiO}_2$  nanoparticles were used. They can reduce swelling of clays and thus improve wellbore stability.

## 2. Laboratory Testing

The impact of adding nanoparticles to a water-based mud on clay swelling was assessed at the Drilling Fluid Laboratory (Department for Petroleum Engineering, Faculty of mining, Geology and Petroleum Engineering, University of Zagreb) in Zagreb, Croatia.

### 2.1. Data on Used Nanoparticles

The nanoparticles used in the laboratory research were  $\text{SiO}_2$  and  $\text{TiO}_2$  nanoparticles. Data on used nanoparticles, which were obtained from their manufacturers, are shown in Table 1.

**Table 1.** Data on  $\text{SiO}_2$  and  $\text{TiO}_2$  nanoparticles from Material Safety Data Sheet (MSDS).

Nanoparticles	$\text{TiO}_2$ -Susp	$\text{SiO}_2$ -Susp
Appearance	Water-based suspension	Water-based suspension
Nanoparticle content	39–41 wt% of Titania suspension ( $\text{TiO}_2$ )	30 wt% of Silica suspension ( $\text{SiO}_2$ )
Average particle size ( $D_{50}$ )	70 nm	120 nm

### 2.2. Composition of Used Aqueous Suspensions and Drilling Mud

To understand the effect of adding nanoparticles, six samples of aqueous suspensions containing  $\text{SiO}_2$  and  $\text{TiO}_2$  nanoparticles were prepared. Nanoparticles were added in three different concentrations: 0.5, 1 and 1.5 wt% (Table 2). To elaborate, a concentration of 0.5 wt% means that in 1000 mL of water, 5 g of  $\text{TiO}_2$  (suspended in 9 mL of  $\text{TiO}_2$ -susp) or  $\text{SiO}_2$  nanoparticles (suspended in 14 mL of  $\text{SiO}_2$ -susp) was added so that their impact on pellet swelling could be compared.

**Table 2.** Composition of aqueous suspensions used in this study.

Aqueous Suspension	Water	Water + $\text{TiO}_2$			Water + $\text{SiO}_2$		
		0.5 wt%	1 wt%	1.5 wt%	0.5 wt%	1 wt%	1.5 wt%
Water	1000 mL	1000 mL	1000 mL	1000 mL	1000 mL	1000 mL	1000 mL
$\text{TiO}_2$ -susp	-	9 mL	18 mL	27 mL	-	-	-
$\text{SiO}_2$ -susp	-	-	-	-	14 mL	28 mL	42 mL

After that, the  $\text{SiO}_2$ -susp and  $\text{TiO}_2$ -susp nanoparticles were added to water-based mud at concentrations of 0.5, 1 and 1.5 wt%. The base mud contained water, 30 g/L bentonite to adjust the rheological properties, 2 g/L of PAC LV polymer to maintain filtration properties and NaOH to adjust the pH value of the base mud (Table 3).

**Table 3.** Composition of drilling muds used in this study.

Mud	Base Mud	Base Mud + $\text{TiO}_2$			Base Mud + $\text{SiO}_2$		
		0.5 wt%	1 wt%	1.5 wt%	0.5 wt%	1 wt%	1.5 wt%
Water	1000 mL	1000 mL	1000 mL	1000 mL	1000 mL	1000 mL	1000 mL
Bentonite	30 g	30 g	30 g	30 g	30 g	30 g	30 g
PAC LV	2 g	2 g	2 g	2 g	2 g	2 g	2 g
NaOH	2 g	2 g	2 g	2 g	2 g	2 g	2 g
$\text{TiO}_2$ -susp	-	9 mL	18 mL	27 mL	-	-	-
$\text{SiO}_2$ -susp	-	-	-	-	14 mL	28 mL	42 mL

After adding the nanoparticles to the base mud, the mixture was stirred for 30 min in a stirrer at a rate of 500 rpm to reduce the agglomeration of nanoparticles and avoid instability of nanoparticle suspensions in drilling muds.

### 2.3. Zeta Potential Measurement

Unstable nanoparticle suspensions usually have high attraction forces that can lead to aggregation of individual nanoparticles into larger particles, which can result in uncontrolled viscosity values or increased filtration [44]. To assess the stability of nanoparticles in the selected muds, the zeta potential of muds containing TiO<sub>2</sub> and SiO<sub>2</sub> nanoparticles was measured. Zeta potential ( $\zeta$ ) was determined by electrophoretic light scattering using a Zetasizer Nano ZS device (Malvern Instruments) equipped with a 532 nm green-light-emitting laser. The zeta potential of the particles was calculated from the measured electrophoretic mobility by means of the Henry equation using the Smoluchowski approximation ( $f(\kappa a) = 1.5$ ). The data processing was performed using the Zetasizer software 7.13 (Malvern Instruments, Malvern, UK). Values of zeta potential above 30 mV or below  $-30$  mV indicate stable suspension because repulsive forces between nanoparticles are strong enough to keep them dispersed in the mud [37,44]. Table 4 shows the calculated values of zeta potential for each stage of preparation of muds containing 0.5 wt% TiO<sub>2</sub> and 0.5 wt% SiO<sub>2</sub> nanoparticles (marked with letters from A to D). In the first stage, zeta potential of bentonite suspension (A) was determined at pH value of 8 and then for each stage after adding a particular additive. By addition of NaOH (C) pH value was increased to 10.5. Mud identified by the letters D and E in Table 4 represent the final formulation of the mud presented in Table 3 referred to as base mud +0.5 wt% TiO<sub>2</sub> and base mud +0.5 wt% SiO<sub>2</sub>. After addition of nanoparticle suspensions to mud C, pH value did not change and amounted to 10.5. Zeta potential was measured six times, and a mean value was taken considering the calculated standard deviation.

**Table 4.** Calculated values of zeta potential.

Measurement No.	Zeta Potential (mV)				
	Bentonite Suspension (A)	A + PAC (B)	B + NaOH (C)	C + 0.5 wt% TiO <sub>2</sub> (D)	C + 0.5 wt% SiO <sub>2</sub> (E)
	pH				
	8	8	10.5	10.5	10.5
1.	-55.4	-59.4	-61.6	-53.5	-51.6
2.	-55.6	-67.1	-63.8	-53.6	-53.8
3.	-64.5	-74.6	-70.7	-54.2	-56.5
4.	-55.1	-59.6	-61.1	-54.5	-51.9
5.	-61.5	-63.4	-63.1	-57.7	-52.4
6.	-68.5	-67.8	-64.7	-57.9	-51.4
<b>Average Value</b>	-60.1	-65.3	-64.2	-55.2	-52.9
<b>Standard Deviation (SD)</b>	5.6	5.8	3.5	2.0	1.9

The measured value of zeta potential for base drilling mud with 0.5 wt% TiO<sub>2</sub> (marked D) is  $-55.2$  mV, and for base drilling mud with 0.5 wt% SiO<sub>2</sub> (marked E) it is  $-52.9$  mV. The obtained values of zeta potential indicate the stability of both drilling muds without nanoparticle aggregation.

### 2.4. Characterization of Bentonite in Pellets

The bentonite used for pellet preparation was Bentonite Tunnel Gel Plus, obtained from the manufacturer Baroid. To determine the particle size distribution and average particle size of bentonite, granulometric analyses were conducted at the Ruđer Bošković Institute in Zagreb.

The selected samples were diluted with deionized water prior to the granulometric analysis to achieve the optimum suspension concentration. Granulometric analyses were performed with the laser beaming method using a LS 13320 (Beckman Coulter, Indianapolis, IN, USA) instrument. A universal

liquid module (ULM) was used for the analysis, ranging from 0.04 to 2000  $\mu\text{m}$ . Each sample was measured in triplicate. Figure 3 shows the average results of three consecutive measurements.

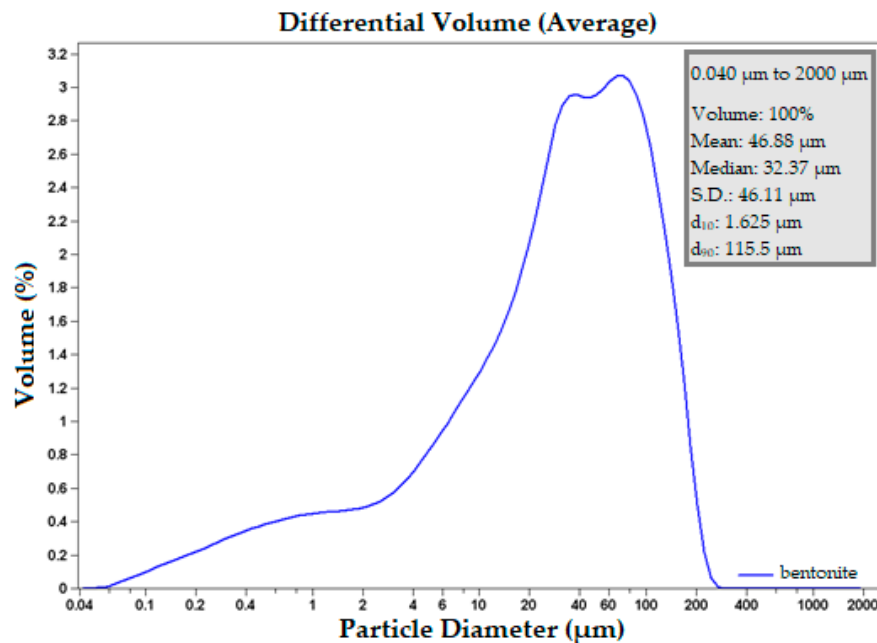


Figure 3. Granulometric curve of bentonite sample.

According to the appearance of the granulometric curve shown in Figure 3, it can be concluded that the Bentonite Tunnel Gel Plus sample shows a very wide distribution, with 75% of the particles ranging from 10 to 300  $\mu\text{m}$ , while the average particle size is 46.9  $\mu\text{m}$ .

### 2.5. Pellet Preparation Procedure and the Swelling Test

During the coring process, real rock samples are obtained on the surface. During drilling through highly reactive clay-rich rocks, which are not reservoir rocks, coring activities represent a significant loss of time and money. Drilling cuttings collected on shale shakers can economically provide valuable geological and petrophysical information in the absence of core data, but the number and quality of these samples are not enough for comprehensive laboratory testing [45]. Because of that, testing on laboratory prepared pellets should be a first step with consequent testing on rock samples, especially clay-rich rocks. Furthermore, laboratory research on pellets provide a better ability to prepare a larger number of samples of completely identical mineral composition and prepared under the same conditions. This allows multiple repetitions of measurements and study of the influence of nanoparticles on artificial rock sample swelling. This approach allows an initial screening procedure for the possible application of nano-based mud in drilling of certain shale formations.

In this study, pellets consisting of bentonite and calcium carbonate in the ratio of 50:50 were used. Pellets were made in a compactor (Figure 4). The compression of samples was performed as follows: A mixture of 6 g of bentonite and 6 g of calcium carbonate was placed in a pre-assembled cell, which was then closed and exposed to the pressure of 41.36 MPa (6000 psi) that remained constant for the subsequent 30 min. The compression pressure and compression times were optimized according to manufacturer's instructions. When selecting the pressure at which the samples were compressed, the type of clay formation that the specific pellets simulated and the conditions to which the clay was exposed in the underground were considered. The compression pressure can be identified using geostatic pressure (pressure of the cap rock) applied on the clay formation at the considered depth. Considering that the average density of rock is 2300  $\text{kg}/\text{m}^3$ , it is possible to calculate the geostatic pressure acting affecting the rock (clay formation) at a certain depth and use this value in laboratory tests. Since the aim of the study was to determine the influence of water-based drilling mud containing



nanoparticles on swelling of soft clay formations located at relatively small depths, a compression pressure of 41.36 MPa (6000 psi) was selected. The selected compression pressure value corresponds to the geostatic pressure value at a depth of approximately 1800 m.

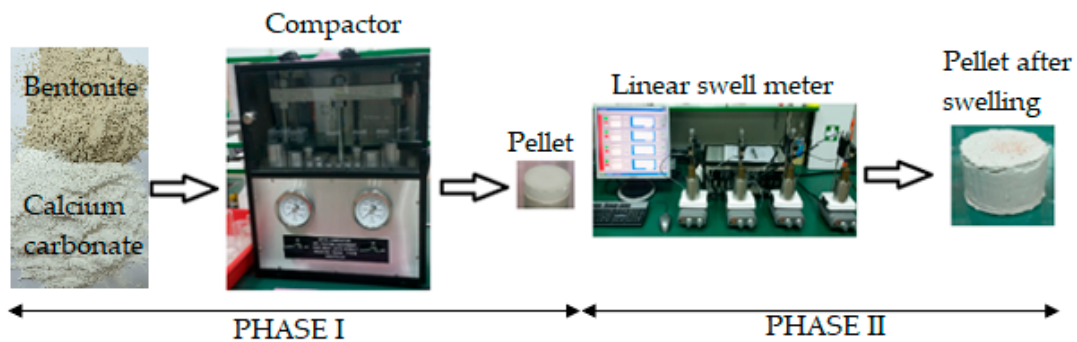


**Figure 4.** Compression of powdered material and testing of pellet swelling.

The swelling test of each pellet in the selected fluid was conceived and conducted as a complete cycle of two phases that lasted for 24.5 h cumulatively. As shown in Figure 4, each cycle consisted of:

- Phase I—30 min compression of powdered material in the compactor (production of pellets);
- Phase II—24 h pellet swelling in the Dynamic Linear Swell Meter.

After the compression time of 30 min had elapsed, pellets were removed from the cell and inserted into Dynamic Linear Swell Meter cell. Swelling was initially carried out using an aqueous solution of nanoparticles at three concentrations (0.5, 1 and 1.5 wt%).

Subsequently, a pellet swelling test was performed in the selected drilling muds. Swelling was measured for 24 h for all pellet samples. The test temperature was 88 °C (192 °F) and the fluid mixing speed was 560 min<sup>-1</sup>.

### 3. Results

Figures 5 and 6 show the swelling of pellets in water and aqueous suspensions that contain SiO<sub>2</sub> nanoparticles (0.5, 1 and 1.5 wt%) expressed in percentages over 2 h (120 min) and 24 h (1440 min). From Figures 5 and 6 it is apparent that the aqueous suspensions of nanoparticles at selected concentrations reduce the swelling of prepared pellets after 2 and 24 h of swelling.

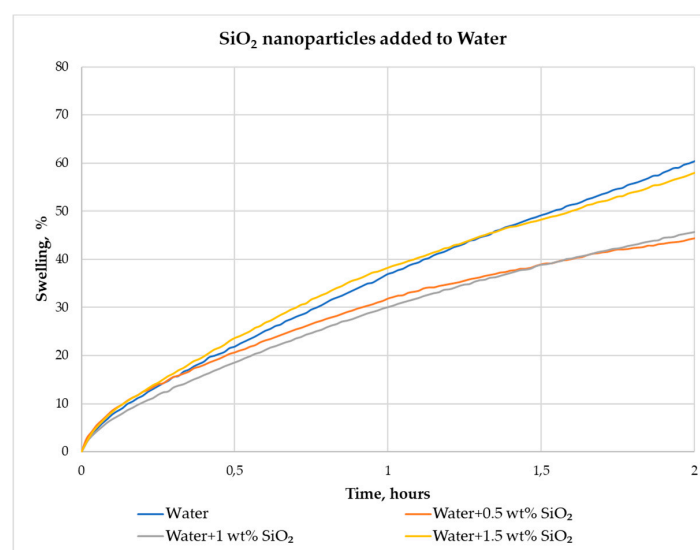


**Figure 5.** The swelling of pellets in water and aqueous suspensions of SiO<sub>2</sub> nanoparticles within 2 h.

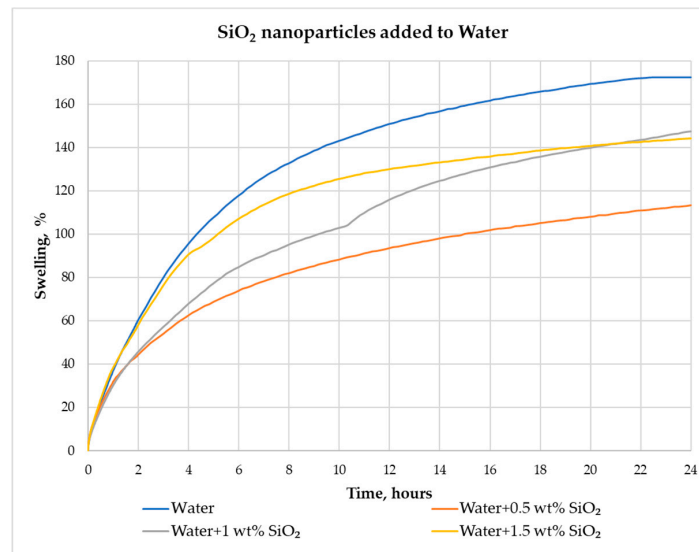
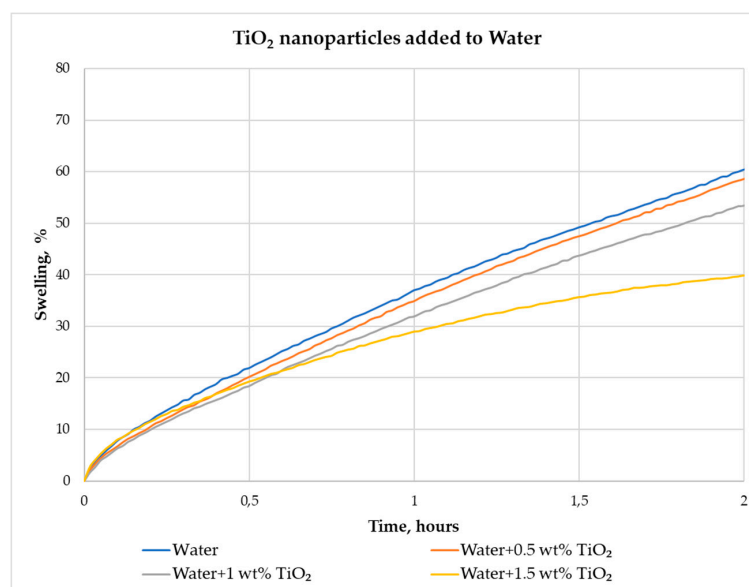


**Figure 6.** The swelling of pellets in water and aqueous suspensions of SiO<sub>2</sub> nanoparticles within 24 h.

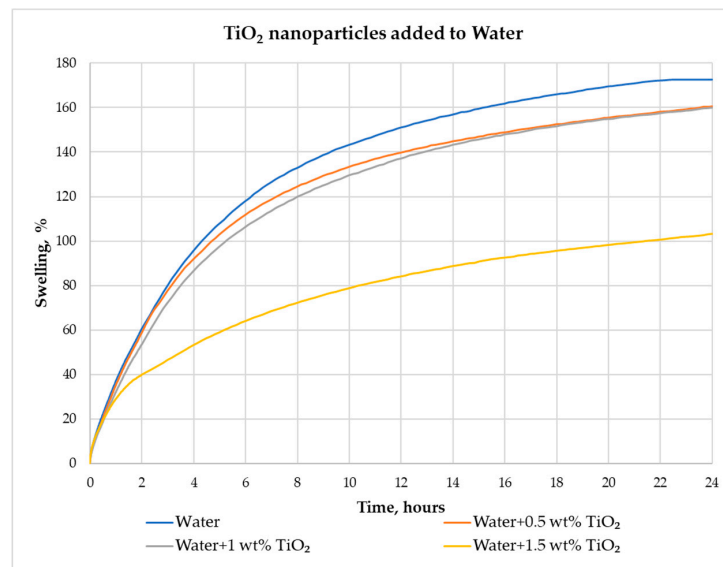
According to Figure 5, the swelling of pellets after 2 h in the aqueous suspension of SiO<sub>2</sub> nanoparticles (0.5 wt%) experienced the most significant reduction of 26.49% compared to their swelling in water. The decrease of pellet swelling in the aqueous suspension of 1 wt% of SiO<sub>2</sub> nanoparticles was slightly less (24.34%) than in aqueous suspension of 0.5 wt% SiO<sub>2</sub> nanoparticles. In the aqueous suspension with 1.5 wt% of SiO<sub>2</sub> nanoparticles, the swelling of pellets was reduced by only 3.97%.

Figure 6 shows that 24 h swelling of pellets in aqueous suspensions at three different concentrations of SiO<sub>2</sub> nanoparticles gives a similar swelling reduction pattern to 2 h. The most significant reduction of pellet swelling was recorded in the aqueous suspension with 0.5 wt% SiO<sub>2</sub> nanoparticles (34.20%) after 24 h. In the aqueous SiO<sub>2</sub> nanoparticle suspension (1 wt%), the swelling was reduced by 14.55% after 24 h, compared to the swelling in water with 1.5 wt% of SiO<sub>2</sub>, which was reduced by 16.41%.

Figures 7 and 8 show the swelling of pellets in water and aqueous suspensions that contain TiO<sub>2</sub> nanoparticles (0.5, 1 and 1.5 wt%) expressed in percentages over 2 h (120 min) and 24 h (1440 min). This was the duration of the entire test. From Figures 7 and 8 it is apparent that aqueous suspensions of TiO<sub>2</sub> nanoparticles at those concentrations reduce the swelling of prepared pellets after 24 h of swelling.



**Figure 7.** The swelling of pellets in water and aqueous suspensions of TiO<sub>2</sub> nanoparticles within 2 h.



**Figure 8.** The swelling of pellets in water and aqueous suspensions of TiO<sub>2</sub> nanoparticles within 24 h.

According to Figure 7, the swelling of pellets after 2 h in an aqueous suspension of 1.5 wt% TiO<sub>2</sub> nanoparticles showed the most significant reduction of 33.94% compared to their swelling in water. In an aqueous suspension of 0.5 wt% of TiO<sub>2</sub> nanoparticles, the swelling of pellets was reduced by only 2.98%, while in an aqueous suspension of 1 wt% of TiO<sub>2</sub> nanoparticles, the decrease of pellet swelling was 11.59%.

Figure 8 shows that the swelling of pellets in aqueous suspensions at two different concentrations of TiO<sub>2</sub> nanoparticles (0.5 and 1 wt%) gives similar results for swelling reduction. In an aqueous TiO<sub>2</sub> nanoparticle suspension (0.5 wt%), after 24 h the swelling was reduced by 6.90% compared to the swelling in water. In the case of the 1 wt% TiO<sub>2</sub>, the swelling was reduced by 7.19%. The best result was recorded in an aqueous TiO<sub>2</sub> nanoparticle suspension (1.5 wt%), where the swelling of pellets was reduced by 40.06%.

Subsequently, SiO<sub>2</sub> nanoparticles and TiO<sub>2</sub> nanoparticles were added to base drilling mud at concentrations of 0.5, 1 and 1.5 wt%, and the swelling pattern was measured for each within 24 h.

Figures 9 and 10 show the swelling of pellets in base mud and in muds with the added SiO<sub>2</sub> nanoparticles, expressed in percentages over 2 h (120 min) and 24 h (1440 min). From Figures 9 and 10 it is apparent that muds containing nanoparticles at selected concentrations reduce the swelling of prepared pellets.

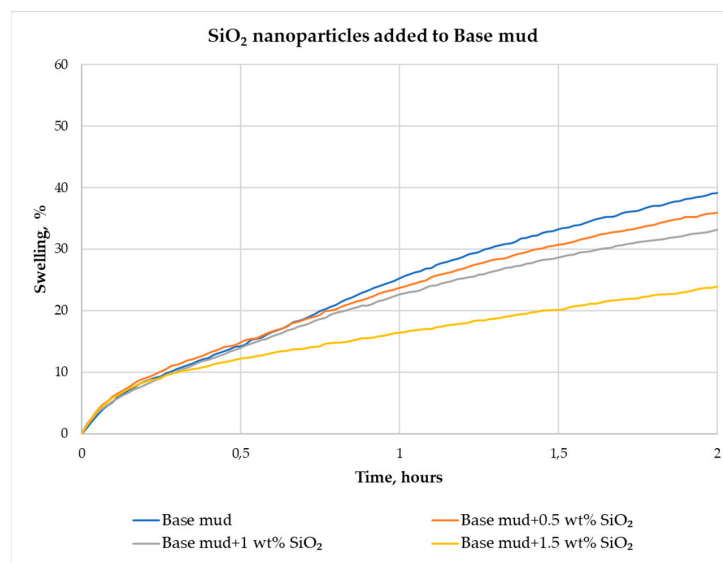


**Figure 9.** Swelling in base mud and in muds with added SiO<sub>2</sub> nanoparticles within 2 h.

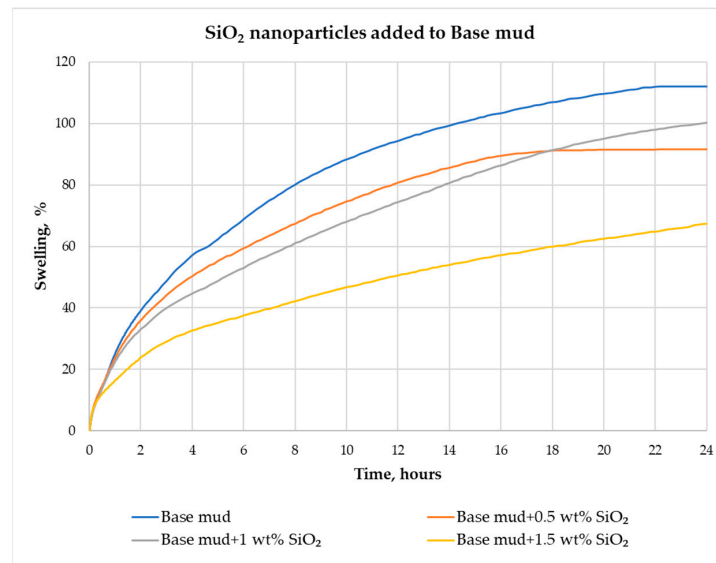


**Figure 10.** Swelling in base mud and in muds with added SiO<sub>2</sub> nanoparticles within 24 h.

According to Figure 9, swelling of pellets after 2 h in mud containing SiO<sub>2</sub> nanoparticles (1.5 wt%) was reduced most significantly, by 38.78%, compared to their swelling in the base mud. In mud containing 0.5 wt% of SiO<sub>2</sub> nanoparticles, the decrease in the swelling of pellets amounted to 8.16%, and in the mud containing 1 wt% of SiO<sub>2</sub> nanoparticles, the swelling of pellets was reduced by 15.31%.

Figure 10 shows that the swelling of pellets after 24 h in the mud containing 1.5 wt% of SiO<sub>2</sub> nanoparticles was reduced the most significantly, by 39.82% compared to their swelling in the base mud. In the mud containing 0.5 wt% of SiO<sub>2</sub> nanoparticles, the decrease was 18.30%, and in the mud containing 1 wt% of SiO<sub>2</sub> nanoparticles, the swelling of pellets was reduced by 10.54%.

Figures 11 and 12 show the swelling of pellets in base mud and in muds with added TiO<sub>2</sub> nanoparticles expressed in percentages within 2 h (120 min) and 24 h (1440 min). From Figures 11 and 12 it is apparent that muds containing nanoparticles at abovementioned concentrations reduce the swelling of the prepared pellets.

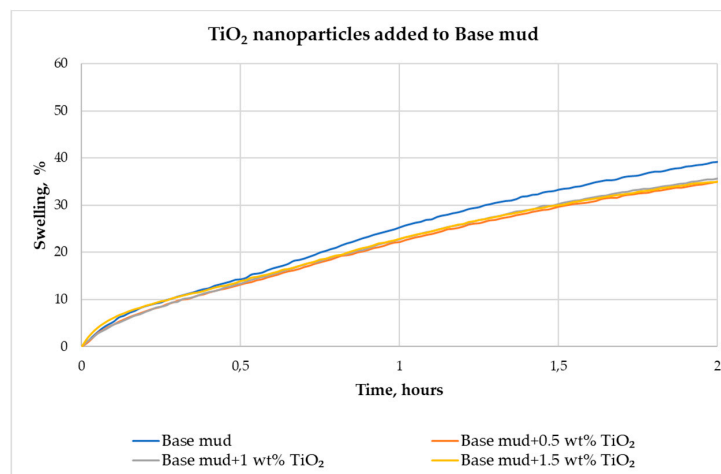


**Figure 11.** Swelling in base mud and in muds with added TiO<sub>2</sub> nanoparticles within 2 h.

According to Figure 11, the swelling of pellets after 2 h in the mud containing TiO<sub>2</sub> nanoparticles in concentrations of 0.5 and 1.5 wt% was reduced by 10.71% compared to their swelling in the base mud. In the mud containing 1 wt% of TiO<sub>2</sub> nanoparticles, the decrease of pallet swelling was 8.93%.

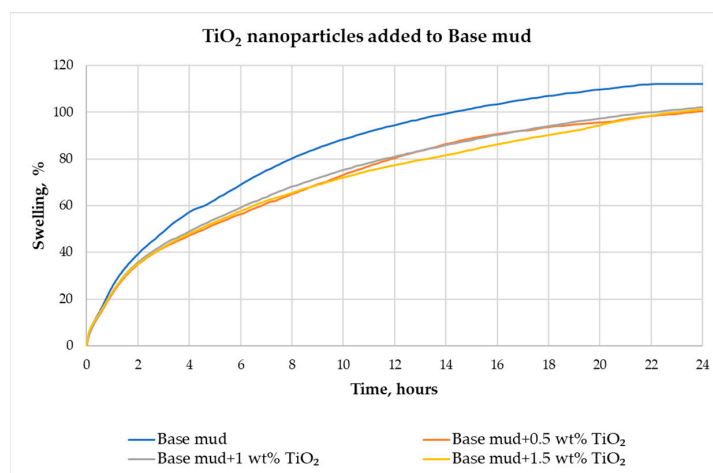


**Figure 12.** Swelling in base mud and in muds with added TiO<sub>2</sub> nanoparticles within 24 h.

Figure 12 shows that swelling of pellets after 24 h in the mud containing 0.5 wt% of TiO<sub>2</sub> nanoparticles was reduced by 10.18% compared to their swelling in the base mud. In mud containing 1 wt% of TiO<sub>2</sub> nanoparticles, the recorded decrease was 8.75% and, in the mud containing 1.5 wt% of TiO<sub>2</sub> nanoparticles, the swelling of pellets was reduced by 9.57%.

After swelling, the pellets were left to be dried, and then SEM images of the pellets were taken (Figure 13).

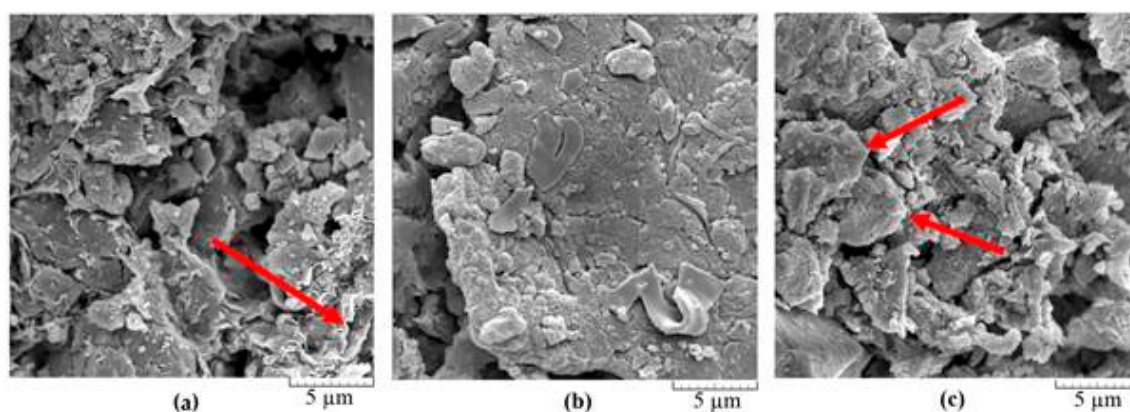


**Figure 13.** A comparison of SEM images of pellets after swelling in basic drilling mud (a), drilling mud with 1 wt% of SiO<sub>2</sub>-susp nanoparticles (b), drilling mud with 1 wt% of TiO<sub>2</sub>-susp nanoparticles (c).

The changes in the structure and texture of the particles are scarcely noticeable in Figure 13a, while clay minerals (mainly Na-montmorillonite) remain relatively recognizable (see arrow). The sample shown in Figure 13b is more compressed, leakproof and more compact than the sample shown in Figure 13a, mainly as an aggregate of slippery particles (less noticeable grain with a recognizable crystal habit). However, it is necessary to determine the chemical composition of the sample and the individual particles in the sample to properly identify the particle type. The sample in Figure 13c resembles the sample swelled in base mud with almost imperceptible modifications to the sample—the morphology of clay minerals and other minerals is mostly undisturbed (arrows show clay minerals aggregates).

#### 4. Discussion

Figures 14 and 15 show a comparison of the results of pellet swelling in different fluids, aqueous suspensions of nanoparticles and water-based muds. These figures outline the results of the laboratory testing after 2 and 24 h.

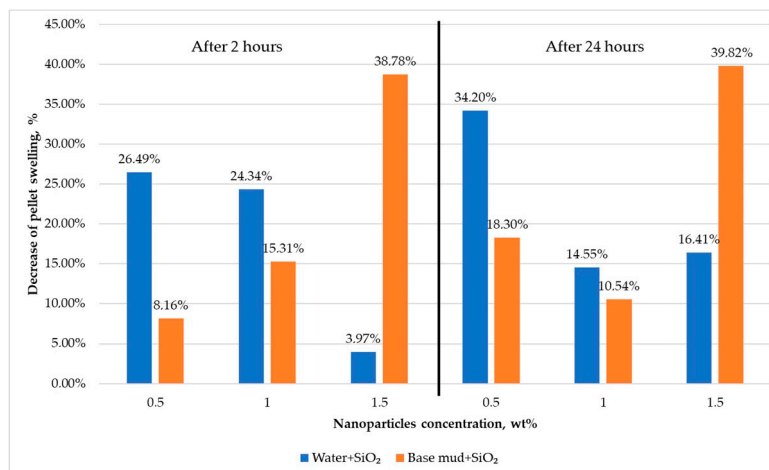


**Figure 14.** Comparison of the results of pellet swelling in different fluids containing SiO<sub>2</sub> nanoparticles after 2 and 24 h.

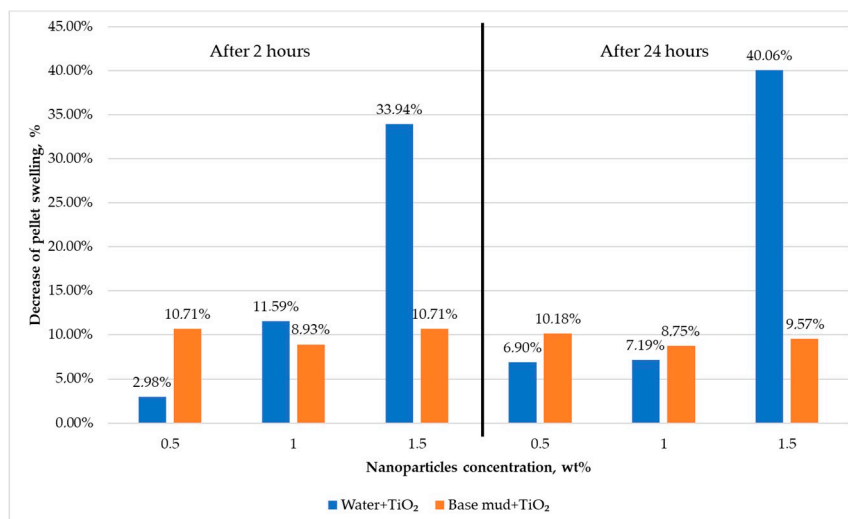


**Figure 15.** Comparison of the results of pellet swelling in different fluids containing TiO<sub>2</sub> nanoparticles after 2 and 24 h.

It was observed that swelling is reduced by adding both types of nanoparticles in the early stage of pellet swelling measurement in an aqueous suspension (2 h), regardless of the concentration of added nanoparticles. After 2 h of pellet swelling in water, the best results were obtained in a TiO<sub>2</sub> aqueous suspension with the 1.5 wt% concentration of nanoparticles (33.94%). After 2 h of pellet swelling in mud, the best result was obtained with SiO<sub>2</sub> nanoparticles added in a concentration of 1.5 wt% to base mud (the decrease in pellet swelling was 38.78%). By addition of TiO<sub>2</sub> nanoparticles to the base mud, similar results of decreasing pellet swelling values were obtained, ranging from 8.93% to 10.71%.

After 24 h of pellet swelling in an aqueous suspension, it was observed that both types of nanoparticles reduce swelling, regardless of the concentration of added nanoparticles. Generally, SiO<sub>2</sub> nanoparticles in aqueous suspension provide better results (less swelling) in relation to TiO<sub>2</sub> nanoparticles at concentrations less than 1 wt%. The best result was obtained with TiO<sub>2</sub> nanoparticles added in a concentration of 1.5 wt% (40.06%). Slightly different results were obtained in the case of swelling in drilling muds with nanoparticles. In this case, similarly to aqueous suspensions of nanoparticles, swelling of pellets decreased in all used muds regardless of the concentration of added nanoparticles. The best results were obtained in the mud for which the SiO<sub>2</sub> nanoparticle

concentration amounted to 1.5 wt% (the decrease in pellet swelling was 39.82%). During pellet swelling in the base mud containing different concentrations of TiO<sub>2</sub> nanoparticles, similar results of decreasing in pellet swelling values were obtained ranging from 8.75% to 10.18%.

As can be seen, the presented results of laboratory research give slightly inconsistent guidelines for possible application of different nanoparticles in drilling fluids for swelling reduction. However, the tested nanoparticles were different in terms of type and size, so they are expected to have different effects on pellet swelling properties. Obviously, the process of swelling reduction depends not only on the type, concentration and size of the added nanoparticles but also on the proportion of other additives in the drilling mud. Moreover, recent research assumes that nanoparticles can plug shale nanopores and thus increase wellbore stability. Still, certain groups of scientists claim that certain forces between nanoparticles and rocks also occur, which could affect results of this study.

Further testing should be focused on the possible interaction between nanoparticles and shale/drilling fluids by gradually increasing the proportion of each additive. Thus, a better insight into the effect of each additive in combination with nanoparticles on the properties of the mud and rock swelling can be obtained. Certainly, after the initial screening process based on results obtained for the linear swell meter, the next step should be performed at elevated pressure and temperature to examine the impact on the effectiveness of nano-based drilling fluids in shale swelling reduction.

## 5. Conclusions

Based on the conducted laboratory research, the following can be concluded:

- The addition of selected SiO<sub>2</sub> and TiO<sub>2</sub> nanoparticles to the water or to the base drilling mud at concentrations of 0.5, 1 and 1.5 wt% reduces swelling of the pellets from 2.98% to 40.06%;
- The swelling of pellets in drilling muds is generally lower than in aqueous suspensions because of the better rheological properties of the mud, which directly reflects on the movement of water into pellets during the swelling process;
- Comparing both types of nanoparticles, better results were obtained by using SiO<sub>2</sub> nanoparticles (D<sub>50</sub> = 120 nm), which are almost two times larger than the TiO<sub>2</sub> nanoparticles (D<sub>50</sub> = 70 nm);
- After 2 and 24 h of pellet swelling in water, the best result was obtained with addition of TiO<sub>2</sub> nanoparticles at a concentration of 1.5 wt% (the swelling reduction was 33.94% and 40.06%, respectively);
- After 2 and 24 h of pellet swelling in the base mud, the best result was obtained with addition of SiO<sub>2</sub> nanoparticles at a concentration of 1.5 wt% (the swelling reduction was 38.78% and 39.82%, respectively).

**Author Contributions:** B.P.—creation of the idea for the paper, preparation of the comprehensive literature overview in the introduction and review of the discussion and conclusion section; N.G.-M.—reviewing the laboratory testing results and writing the discussion and conclusion section; P.M.—writing pellet preparation procedure section and the swelling test, laboratory testing and preparation of the figures in laboratory testing section; I.M.—preparation of the zeta potential measurements and characterization of bentonite in pellets, laboratory testing and preparation of the laboratory testing results. All authors have read and agreed to the published version of the manuscript.

**Funding:** This research received no external funding.

**Conflicts of Interest:** The authors declare no conflict of interest.

## References

1. Qu, Y.; Lai, X.; Zou, L.; Su, Y. Polyoxyalkylamine as Shale Inhibitor in Water-Based Drilling Fluids. *Appl. Clay Sci.* **2009**, *44*, 265–268. [[CrossRef](#)]
2. Gaurina-Međimurec, N.; Pašić, B. Risk Due to Wellbore Instability. In *Risk Analysis for Prevention of Hazardous Situations in Petroleum and Natural Gas Engineering*; Matanović, D., Gaurina-Međimurec, N., Simon, K., Eds.; IGI Global: Hershey, PA, USA, 2014; pp. 23–46.
3. Albooyeh, M.; Rahimzadeh Kivi, I.; Ameri, M. Promoting wellbore stability in active shale formations by water-based muds: A case study in Pabdeh shale, Southwestern Iran. *J. Nat. Gas Sci. Eng.* **2018**, *56*, 166–174. [[CrossRef](#)]

4. Chen, X.; Tan, C.P.; Haberfield, C.M. A Comprehensive, Practical Approach for Wellbore Instability Management. *SPE Drill. Complet.* **2002**, *17*, 224–236. [[CrossRef](#)]
5. Pašić, B.; Gaurina-Međimurec, N.; Matanović, D. Wellbore Instability: Causes and Consequences. *Min.-Geol.-Pet. Eng. Bull.* **2007**, *19*, 87–98.
6. Kumar, R.; Al Busaidi, S.; Al Ghafri, A.M.D.; Al Amri, A.; Uwe, J.S.; Khaldi, S. Wellbore Stability and Hole Cleaning Management for Successful Well Design Optimization in Deep Tight Gas Field. In Proceedings of the SPE/IADC Middle East Drilling Technology Conference and Exhibition, Abu Dhabi, UAE, 29–31 January 2018. [[CrossRef](#)]
7. Reyes, A.; Huang, J.J.; Yuan, Z.; Temple, P.; Liang QMorana, J.; Hashemian, Y. Cloud-Based Coherent Wellbore Stability, Improving Trajectory Design for Unconventional Well Construction Planning. In Proceedings of the IADC/SPE International Drilling Conference and Exhibition, Galveston, TX, USA, 3–5 March 2020. [[CrossRef](#)]
8. Haider, M.Q.; Abbas, A.K.; Haider, D.H. Wellbore Instability Analysis for Nahr Umr Formation in Southern Iraq. In Proceedings of the 52nd US Rock Mechanics/Geomechanics Symposium, Seattle, WA, USA, 17–20 June 2018.
9. Gholami, R.; Elochukwu, H.; Fakhari, N.; Sarmadivaleh, M. A review on borehole instability in active shale formations: Interactions, mechanisms and inhibitors. *Earth-Sci. Rev.* **2018**, *177*, 2–13. [[CrossRef](#)]
10. Subbiah, S.K.; Povstyanova, M.; Egawa, S.; Kukubo, S.; Yahata, K.; Okuzawa, T.; Vantala, A.; Tan, C.P.; Nasreldin, G.; Martin, J.W.; et al. Chemo-Mechanical Behavior for UAE Shales and Mud Design for Wellbore Stability. In Proceedings of the Abu Dhabi International Petroleum Exhibition & Conference, Abu Dhabi, UAE, 12–15 November 2018. [[CrossRef](#)]
11. Aftab, A.; Ismail, A.R.; Ibupoto, Z.H. Enhancing the rheological properties and shale inhibition behavior of water-based mud using nanosilica, multi-walled carbon nanotube, and graphene nanoplatelet. *Egypt. J. Pet.* **2017**, *26*, 291–299. [[CrossRef](#)]
12. Anderson, R.L.; Ratcliffe, I.; Greenwell, H.C.; Williams, P.A.; Cliffe SCoveney, P.V. Clay swelling—A challenge in the oilfield. *Earth-Sci. Rev.* **2010**, *98*, 201–216. [[CrossRef](#)]
13. Ali, M.; Jarni, H.H.; Aftab, A.; Ismail, A.R.; Saady, N.M.C.; Sahito, M.F.; Keshavarz, A.; Iglauer, S.; Sarmadivaleh, M. Nanomaterial-based drilling fluids for exploitation of unconventional reservoirs: A review. *Energies* **2020**, *13*, 3417. [[CrossRef](#)]
14. Yue, Y.; Chen, S.; Wang, Z.; Yang, X.; Peng, Y.; Cai, J.; Nasr-El-Din, H.A. Improving wellbore stability of shale by adjusting its wettability. *J. Pet. Sci. Eng.* **2018**, *161*, 692–702. [[CrossRef](#)]
15. Parkash, D.; Deangeli, C. Wellbore Stability Analysis in Anisotropic Shale Formations. In Proceedings of the SPE/PAPG Pakistan Section Annual Technical Symposium and Exhibition, Islamabad, Pakistan, 18–20 November 2019. [[CrossRef](#)]
16. Adewole, J.K.; Kazeem, T.S.; Oyehan, T.A. Molecular Transport of Solutes and Ions Through Filter-Cake: Implications for Wellbore Instability and Formation Damage. In Proceedings of the SPE Kingdom of Saudi Arabia Annual Technical Symposium and Exhibition, Dammam, Saudi Arabia, 23–26 April 2018. [[CrossRef](#)]
17. Patel, A.; Stamatakis, E.; Young, S.; Friedheim, J. Advances in Inhibitive Water-Based Drilling Fluids—Can They Replace Oil-Based Muds? In Proceedings of the SPE International Symposium on Oilfield Chemistry, Houston, TX, USA, 28 February–2 March 2007. [[CrossRef](#)]
18. Berry, S.L.; Boles, J.L.; Brannon, H.D.; Beall, B.B. Performance Evaluation of Ionic Liquids as a Clay Stabilizer and Shale Inhibitor. In Proceedings of the SPE International Symposium and Exhibition on Formation Damage Control, Lafayette, LA, USA, 13–15 February 2018. [[CrossRef](#)]
19. Hussein, A.H.; Al-Khaja, M.J.; Al-Menayes, F.; Al-Haddad, H.; Malik, A.A.A.; Durge, A.; Dashti, R.; Abdelaziz, R.M.; Barsoum, V.; Aleem, B.A.; et al. The Application of Chemistry to Manage Wellbore Instability While Drilling the Mechanically Weak Burgan Shale Formation and the Vugular Shuaiba Limestone Formation. In Proceedings of the SPE International Heavy Oil Conference and Exhibition, Kuwait City, Kuwait, 10–12 December 2018. [[CrossRef](#)]
20. Haddad, H.; Al-Khaja, M.J.; Saffar, A.H.; Raturi, S.K.; Aleem, B.A.; Samak, M.; ElSeheemy, E.I.; Barsoum, V.; Abdelaziz, R.; Rockwood, J. Conquering Wellbore Instability in Kuwait. In Proceedings of the SPE Kuwait Oil & Gas Conference and Show, Mishref, Kuwait, 13–16 October 2019. [[CrossRef](#)]



21. Kumar, S.; Sundriyal, P.; Kumar, N. Formulation of Inhibitive Water Based Mud System with Synthesized Graft Copolymer: A Novel Approach to Mitigate the Wellbore Instability Problems in Shale Formation. In Proceedings of the Abu Dhabi International Petroleum Exhibition & Conference, Abu Dhabi, UAE, 13–16 November 2017. [\[CrossRef\]](#)
22. Long, L.; Xianguang, X.; Jinsheng, S.; Xubo, Y.; Yingmin, L. Vital Role of Nanomaterials in Drilling Fluid and Reservoir Protection Applications. In Proceedings of the Abu Dhabi International Petroleum Exhibition & Conference, Abu Dhabi, UAE, 11–14 November 2012. [\[CrossRef\]](#)
23. Aftab, A.; Ali, M.; Sahito, M.F.; Mohanty, U.S.; Jha, N.K.; Akhondzadeh, H.; Azhar, M.R.; Ismail, A.R.; Keshavarz, A.; Iglauer, S. Environmental Friendliness and High Performance of Multifunctional Tween 80/ZnO-Nanoparticles-Added Water-Based Drilling Fluid: An Experimental Approach. *ACS Sustain. Chem. Eng.* **2020**, *8*, 11224–11243. [\[CrossRef\]](#)
24. Borisov, A.S.; Husein, M.; Hareland, G. A Field Application of Nanoparticle-Based Invert Emulsion Drilling Fluid. *J. Nanoparticle Res.* **2015**, *17*, 1–13. [\[CrossRef\]](#)
25. Singh, H.; Yadav, P.; Imtiaz, S.; Perumalla, S. Resolving Shale Drilling Instabilities in the Middle East: A Holistic & Pragmatic Geomechanical Methods. In Proceedings of the Abu Dhabi International Petroleum Exhibition & Conference, Abu Dhabi, UAE, 13–16 November 2017. [\[CrossRef\]](#)
26. Al-Ajmi, A.M.; Al-Rushoud, A.S.; Gohain, A.K.; Al-Haj, H.A.; Khatib, F.I.; Al-Mutawa, F.M.; Al-Gharib, M.A.; Soliman, A.H.; Ibrahim, A.S.; Al-Mujalhem, M.Q. Nontechnology Improves Wellbore Strengthening and minimized Differential Sticking Problems in High Depleted Formations. In Proceedings of the Abu Dhabi International Petroleum Exhibition & Conference, Abu Dhabi, UAE, 7–10 November 2016. [\[CrossRef\]](#)
27. Chengyun, M.; Jingen, D.; Baohua, Y.; Sen, L.; Hai Tao, L. Effective Improvement of Wellbore Stability in Shales with a Novel Nanocomposite. In Proceedings of the 51st US Rock Mechanics/Geomechanics Symposium, San Francisco, CA, USA, 25–28 June 2017.
28. Cai, J.; Chenevert, M.E.; Sharma, M.M.; Friedheim, J.E. Decreasing Water Invasion into Atoka Shale Using Nonmodified Silica Nanoparticles. *SPE Drill. Complet.* **2012**, *27*, 103–112. [\[CrossRef\]](#)
29. Patil, R.C.; Deshpande, A. Use of Nanomaterials in Cementing Applications. In Proceedings of the SPE International Oilfield Nanotechnology Conference and Exhibition, Noordwijk, the Netherlands, 12–14 June 2012. [\[CrossRef\]](#)
30. Hoelscher, K.P.; De Stefano, G.; Riley, M.; Young, S. Application of Nanotechnology in Drilling Fluids. In Proceedings of the SPE International Oilfield Nanotechnology Conference and Exhibition, Noordwijk, the Netherlands, 12–14 June 2012. [\[CrossRef\]](#)
31. Caldarola, V.T.; Akhtarmanesh, S.; Cedola, A.E.; Qader, R.; Hareland, G. Potential Directional Drilling Benefits of Barite Nanoparticles in Weighted Water-based Drilling Fluids. In Proceedings of the 50th US Rock Mechanics/Geomechanics Symposium, Houston, TX, USA, 26–29 June 2016.
32. Gao, C.; Miska, S.Z.; Yu, M.; Ozbayoglu, E.M.; Takach, N.E. Effective Enhancement of Wellbore Stability in Shales with New Families of Nanoparticles. In Proceedings of the SPE Deepwater Drilling & Completions Conference, Galveston, TX, USA, 14–15 September 2016. [\[CrossRef\]](#)
33. Wang, X.; Chen, M.; Jin, Y.; Lu, Y.; Yang, S. Decreasing Water Invasion into Shale Using Hydrophilic Sulfonated Silica Nanoparticles. In Proceedings of the 52nd US Rock Mechanics/Geomechanics Symposium, Seattle, WA, USA, 17–20 June 2018.
34. Amanullah, M.; Al-Tahini, A.M. Nano-technology-its significance in smart fluid development for oil and gas field application. In Proceedings of the SPE Saudi Arabia Section Technical Symposium, Al-Khobar, Saudi Arabia, 9–11 May 2009. [\[CrossRef\]](#)
35. El-Diasty, A.I.; Ragab, A.M.S. Applications of nanotechnology in the oil & gas industry: Latest trends worldwide & future challenges in Egypt. In Proceedings of the North Africa Technical Conference and Exhibition, Cairo, Egypt, 15–17 April 2013. [\[CrossRef\]](#)
36. Aftab, A.; Ali, M.; Arif, M.; Panhwar, S.; Saady, N.M.C.; Al-Khdheewi, E.A.; Mahmoud, O.; Ismail, A.R.; Keshavarz, A.; Iglauer, S. Influence of tailor-made TiO<sub>2</sub>/API bentonite nanocomposite on drilling mud performance: Towards enhanced drilling operations. *Appl. Clay Sci.* **2020**, *199*. [\[CrossRef\]](#)
37. Hoxha, B.B.; van Oort, E.; Daigle, H. How Do Nanoparticles Stabilize Shale? *SPE Drill. Complet.* **2017**, *34*, 143–158. [\[CrossRef\]](#)
38. Irfan, Y. Study of Viscosity and Friction Factor of Nano Drilling Fluids along with Torque and Drag Reduction. Master's Thesis, Faculty of Science and Technology, University of Stavanger, Stavanger, Norway, 2016; p. 128.

39. Mijić, P.; Gaurina-Međimurec, N.; Pašić, B. The Influence of SiO<sub>2</sub> and TiO<sub>2</sub> Nanoparticles on the Properties of Water-Based Mud. In Proceedings of the 36th International Conference on Ocean, Offshore and Arctic Engineering, American Society of Mechanical Engineers, Trondheim, Norway, 25–30 June 2017. [CrossRef]
40. ShamsiJazeyi, H.; Miller, C.A.; Wong, M.S.; Tour, J.M.; Verduzco, R. Polymer-coated nanoparticles for enhanced oil recovery. *J. Appl. Polym. Sci.* **2014**, *131*. [CrossRef]
41. Roustaei, A.; Bagherzadeh, H. Experimental investigation of SiO<sub>2</sub> nanoparticles on enhanced oil recovery of carbonate reservoirs. *J. Pet. Explor. Prod. Technol.* **2015**, *5*, 27–33. [CrossRef]
42. Bahraminejad, H.; Khaksar Manshad, A.; Riazi, M.; Ali, J.A.; Sajadi, S.M.; Keshavarz, A. CuO/TiO<sub>2</sub>/PAM as a Novel Introduced Hybrid Agent for Water—Oil Interfacial Tension and Wettability Optimization in Chemical Enhanced Oil Recovery. *Energy Fuels* **2019**, *33*, 10547–10560. [CrossRef]
43. Asl, H.F.; Zargar, G.; Manshad, A.K.; Takassi, M.A.; Ali, J.A.; Keshavarz, A. Effect of SiO<sub>2</sub> nanoparticles on the performance of L-Arg and L-Cys surfactants for enhanced oil recovery in carbonate porous media. *J. Mol. Liq.* **2020**, *300*, 112290. [CrossRef]
44. Aramendiz, J.; Imqam, A.; Fakher, S.M. Design and Evaluation of a Water-Based Drilling Fluid Formulation Using SiO and Graphene Oxide Nanoparticles for Unconventional Shales. In Proceedings of the International Petroleum Technology Conference, Beijing, China, 1–17 March 2019. [CrossRef]
45. Pašić, B.; Gaurina-Međimurec, N.; Mijić, P.; Barudžija, U. Application of Outcrops Rock Samples in Laboratory Research of Shale Drilling Fluid Interaction. In Proceedings of the 36th International Conference on Ocean, Offshore and Arctic Engineering, American Society of Mechanical Engineers, Trondheim, Norway, 25–30 June 2017. [CrossRef]

**Publisher’s Note:** MDPI stays neutral with regard to jurisdictional claims in published maps and institutional affiliations.



© 2020 by the authors. Licensee MDPI, Basel, Switzerland. This article is an open access article distributed under the terms and conditions of the Creative Commons Attribution (CC BY) license (<http://creativecommons.org/licenses/by/4.0/>).